Defect and Diffusion Forum *Online: 2007-09-04*
ISSN: 1662-9507, Vol. 266, pp 191-198
doi:10.4028/www.scientific.net/DDF.266.191

Interdiffusion in (fcc) Ni-Cr-X (X = Al, Si, Ge or Pd) Alloys at 700°C

N. Garimella[1, a], M.P. Brady[2, b] and Y.H. Sohn[1, c]

[1]Advanced Materials Processing and Analysis Center and Department of Mechanical, Materials and Aerospace Engineering, University of Central Florida, Orlando, FL, USA.

[2]Metals and Ceramics Division, Oak Ridge National Laboratory, Oak Ridge, TN, USA.

[a]garimella_n@yahoo.com, [b] bradymp@ornl.gov, [c] ysohn@mail.ucf.edu

Keywords: Boltzmann/Matano analysis, diffusion couples, diffusion coefficients, experimental, interdiffusion, multicomponent alloys, ternary system.

Abstract. Interdiffusion at 700°C for Ni-22at.%Cr (fcc γ phase) alloys with small additions of Al, Si, Ge, or Pd was examined using solid-to-solid diffusion couples. Rods of Ni-22at.%Cr, Ni-21at.%Cr-6.2at.%Al, Ni-22at.%Cr-4.0at.%Si, Ni-22at.%Cr-1.6at.%Ge and Ni-22at.%Cr-1.6at.%Pd alloys were cast using arc-melt and homogenized at 900°C for 168 hours. The diffusion couples were assembled with alloy disks in Invar steel jig, encapsulated in Argon after several hydrogen flushes, and annealed at 700°C for 720 hours. Experimental concentration profiles were determined from polished cross-sections by using electron probe microanalysis with pure standards of Ni, Cr, Al, Si, Ge and Pd. Interdiffusion fluxes of individual components were calculated directly from the experimental concentration profiles, and the moments of interdiffusion fluxes were examined to determine average ternary interdiffusion coefficients. Effects of ternary alloying additions on the interdiffusional behavior of Ni-Cr-X alloys at 700°C are presented in the light of the diffusional interactions and the formation of protective Cr_2O_3 scale.

Introduction

Ni-Cr alloys have been extensively explored for a variety of high-temperature applications and form a basis for a numerous commercial superalloy families [1-3]. They possess a good oxidation resistance and excellent high-temperature strength. Oxidation resistance in these alloys is derived from a continuous, slow-growing, adherent Cr_2O_3 scale [1-3]. Minor alloying additions (< 6.2at.%) can significantly improve the oxidation resistance of these Cr_2O_3 forming alloys although the exact mechanism by which the improvement occurs requires further investigation [1,4-6]. Diffusional influence from minor alloying additions can play a significant role in assessing the oxidation behavior of these alloys [1-8]. Ternary interdiffusion coefficients are important parameters to elucidate the effects of minor alloying additions on the oxidation of Cr_2O_3-forming alloys.

In this work, interdiffusion in Ni-22at.%Cr-X (fcc γ phase) alloys (X = Al, Si, Ge, or Pd) was examined using solid-to-solid diffusion couples annealed at 700°C for 720 hours. The selection basis of minor alloying additions (e.g., Al, Si, Ge and Pd) has been described in previous interdiffusion study carried out at 900°C [9]. Experimental concentration profiles are employed to calculate interdiffusion fluxes of individual components, and to determine average effective interdiffusion coefficients and average ternary interdiffusion coefficients. Interdiffusion coefficients are examined to assess the influence of alloying additions on the interdiffusion behavior of Cr and the Cr_2O_3-forming ability in Ni-22at.%Cr alloys.

Determination of Interdiffusion Coefficients from Ternary Isothermal Diffusion Couples

On the basis of Onsager's formalism [10], the interdiffusion flux $\widetilde{J}_i$ of a component i in a ternary system can be written as:

$$\widetilde{J}_i = -\widetilde{D}^3_{i1}\frac{\partial C_1}{\partial x} - \widetilde{D}^3_{i2}\frac{\partial C_2}{\partial x} \quad (i, j = 1,2) \tag{1}$$

where $\partial C_1/\partial x$ and $\partial C_2/\partial x$ are the two independent concentration gradients, and $\widetilde{D}^3_{i1}$ and $\widetilde{D}^3_{i2}$ are the ternary interdiffusion coefficients. An experimental determination of the four concentration dependent interdiffusion coefficients requires the use of the Boltzmann-Matano analysis with two independent diffusion couples intersecting at a common composition in the diffusion zone.

Alternatively, the interdiffusion fluxes $\widetilde{J}_i$ of all components can be determined directly from their concentration profiles of an infinite diffusion couple without the need of the interdiffusion coefficients using the expression [11]:

$$\widetilde{J}_i = \frac{1}{2t}\int_{C_i^- \text{ or } C_i^+}^{C_i(x)} (x - x_o)\,dC_i \quad (i = 1, 2, ..., n) \tag{2}$$

where t is the time, C_i^- and C_i^+ are the terminal concentrations of the alloys employed for the couple and x_o refers to the location of the Matano plane. The interdiffusion flux $\widetilde{J}_i$ can then be integrated with respect to position x to define average effective interdiffusion coefficient $\tilde{D}_i^{eff}$ [12]:

$$\tilde{D}_i^{eff} = \frac{\int_{x_1}^{x_2} \tilde{J}_i dx}{C_i^{x_2} - C_i^{x_1}} \quad (i = 1,2,3) \tag{3}$$

The effective interdiffusion coefficient is a chemical diffusion coefficient of individual species and it incorporates all multicomponent diffusional interactions within the system to provide an effective value for the interdiffusion of a component species as defined by:

$$\widetilde{D}_i^{eff} = \widetilde{D}_{ii}^n + \sum_j^{n-1} \frac{\widetilde{D}_{ij}^n \partial C_j / \partial x}{\partial C_i / \partial x} (i \neq j) \tag{4}$$

The interdiffusion flux $\widetilde{J}_i$ can be multiplied by $(x\text{-}x_o)^m$ and integrated over a selected region, x_1 to x_2 one gets [13]:

$$\int_{x_1}^{x_2} \widetilde{J}_i (x - x_o)^m dx = -\overline{\widetilde{D}}^3_{i1} \int_{C_1(x_1)}^{C_1(x_2)} (x - x_o)^m dC_1 - \overline{\widetilde{D}}^3_{i2} \int_{C_2(x_1)}^{C_2(x_2)} (x - x_o)^m dC_2 \quad (i, j = 1,2) \tag{5}$$

where $\overline{\widetilde{D}}^3_{ij}$ $(i, j = 1,2)$ coefficients are the average main and cross interdiffusion coefficients treated as constants over the selected composition range. For ternary interdiffusion with the independent components and infinitely possible moments (e.g., m=0, 1, 2, …), Eq. 5 can provide, at least, four equations involving the four interdiffusion coefficients $\overline{\widetilde{D}}^3_{ij}$. The $\overline{\widetilde{D}}^3_{ij}$ coefficients, characteristic

representations of the diffusion path, can be determined over selected composition ranges that include nonlinear segment of the profiles [13].

Experimental Procedure

Binary and ternary Ni-Cr-X alloys (fcc γ phase) with compositions reported in Table 1 were prepared with 99.9% pure Ni, Cr, Al, Si, Ge and Pd by arc melting under an argon atmosphere. The alloys were chill-cast by water-cooled copper mold into rods with approximately 12 mm in diameter. The alloy rods were placed in a quartz capsules, evacuated to a pressure less than 10^{-6} torr, and flushed several times with hydrogen. Ar was filled into the quartz capsules before the final sealing. All these alloy rods enclosed in quartz capsule assemblies, were homogenized at 900°C for 168 hours in a horizontal Lindberg™ 3-zone tube furnace, and water-quenched to preserve the high temperature microstructure. The microstructures and compositions of the alloys were examined by optical microscopy, scanning electron microscopy (SEM), energy dispersive spectroscopy (EDS) and electron microprobe analysis (EPMA). No measurable deviation in the alloy compositions was observed, and all alloys consisted of single phase fcc Ni solid solution (γ-phase).

Table 1. Nominal compositions of Ni-Cr-X alloys employed for solid-to-solid diffusion couples.

Alloy Identification	Composition (atom fraction)			Composition (weight fraction)		
	Ni	Cr	X	Ni	Cr	X
Ni	100.0	-	-	100	-	-
Ni-Cr (X = None)	78.0	22.0	-	80	20	-
Ni-Cr-Al (X = Al)	72.5	21.3	6.2	77	20	3
Ni-Cr-Si (X = Si)	74.0	22.0	4.0	78	20	2
Ni-Cr-Ge (X = Ge)	76.3	22.1	1.6	78	20	2
Ni-Cr-Pd (X = Pd)	76.1	22.3	1.6	77	20	3

Diffusion disks with approximate thickness of 2 mm were sliced from the alloy rods and prepared metallographically by polishing through 0.25 μm diamond paste. Table 2 presents ternary diffusion couples that were assembled with the disks held together in Invar™ steel jig consisting of two end plates and three threaded rods. The couples were placed in quartz capsules, which were sealed at one end, evacuated to a pressure less than 10^{-6} torr, and flushed with hydrogen several times. Ar was filled into a capsule before the final sealing. The capsules containing the couples were annealed at 700˚C in a horizontal Lindberg 3-zone furnace for 720 hours. After the anneal, the couples were quenched in water to avoid any compositional and/or microstructural changes.

Table 2. List of solid-to-solid diffusion couples annealed at 700°C for 720 hours.

Series	Diffusion Couples
I	Ni vs. Ni-Cr
II	Ni vs. Ni-Cr-Al
	Ni vs. Ni-Cr-Si
	Ni vs. Ni-Cr-Ge
	Ni vs. Ni-Cr-Pd
III	Ni-Cr vs. Ni-Cr-Al
	Ni-Cr vs. Ni-Cr-Si
	Ni-Cr vs. Ni-Cr-Ge
	Ni-Cr vs. Ni-Cr-Pd

The diffusion couple assembly was then mounted, cross-sectioned, metallographically prepared for microstructural observations. Excellent bonding was observed with all diffusion couples. Then, cross-section surface was repolished with 1μm diamond paste for electron probe microanalysis (EPMA). The concentration profiles of elements Ni, Cr, Al, Si, Ge and Pd for the diffusion couples were determined with a JEOL 733 (Tokyo, Japan) EPMA by point-to-point counting techniques using pure Ni, Cr, Al, Si, Ge, and Pd as standards. Intensities of K_α X-radiations for Ni, Cr, Al, Si, Ge, and L_α X-radiations for Pd were measured and converted to their respective concentrations with appropriate ZAF (atomic number, Z; absorption, A; fluorescence, F) corrections.

Concentration profiles obtained from EPMA were smoothened by a smoothing-spline approximation using MatLab (The Math Works, Natick, MA). It is worth to mention that the analytical method used to determine interdiffusion coefficients in this study, is by the integration of interdiffusion fluxes (e.g., Eq. 5). This does not require the use of concentration gradients and therefore it significantly reduces the influence of a smoothening procedure on the determination of interdiffusion coefficients.

Results and Discussions

Excellent diffusion bonding was achieved in all diffusion couples. Fig. 1 presents a typical optical micrograph obtained by etching (Kalling's reagent) the polished surface of the diffusion couple.

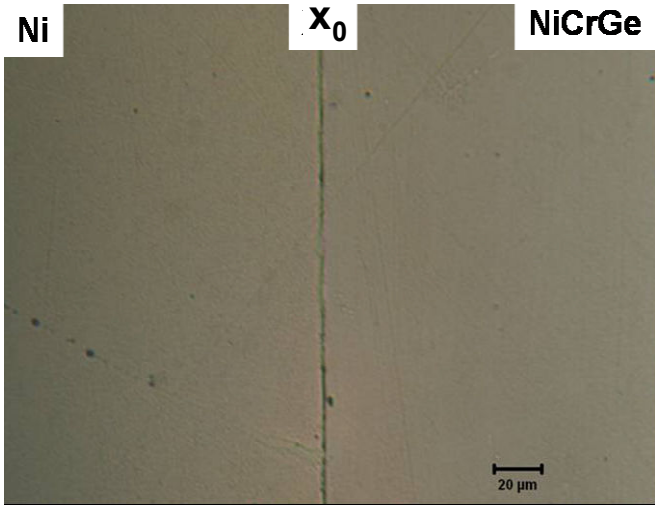

Fig. 1. Typical optical micrograph of solid-to-solid diffusion couple Ni vs. Ni-Cr-Ge annealed at 700°C for 720 hours.

Fig. 2 presents an example of experimental and smoothened concentration profiles that were used for the determination of interdiffusion fluxes and interdiffusion coefficients. The scatters in the concentration profiles for all diffusion couples were within the experimental uncertainty associated with EPMA. Experimental concentration profiles were smoothened with a smoothing-spline approximation by using MatLab. Consistency in experimental and smoothened concentration profiles of Cr in series III (see for example Fig. 2), owing to similar terminal concentration was examined by multiple EPMA acquisitions (e.g., independent Cr concentration) and by close examination of concentration profiles for Ni and X ternary alloying additions (e.g., dependent Cr concentrations). *Consistency in terms of repeatable assessment of all concentration profiles was obtained for determination of interdiffusion fluxes and interdiffusion coefficients.*

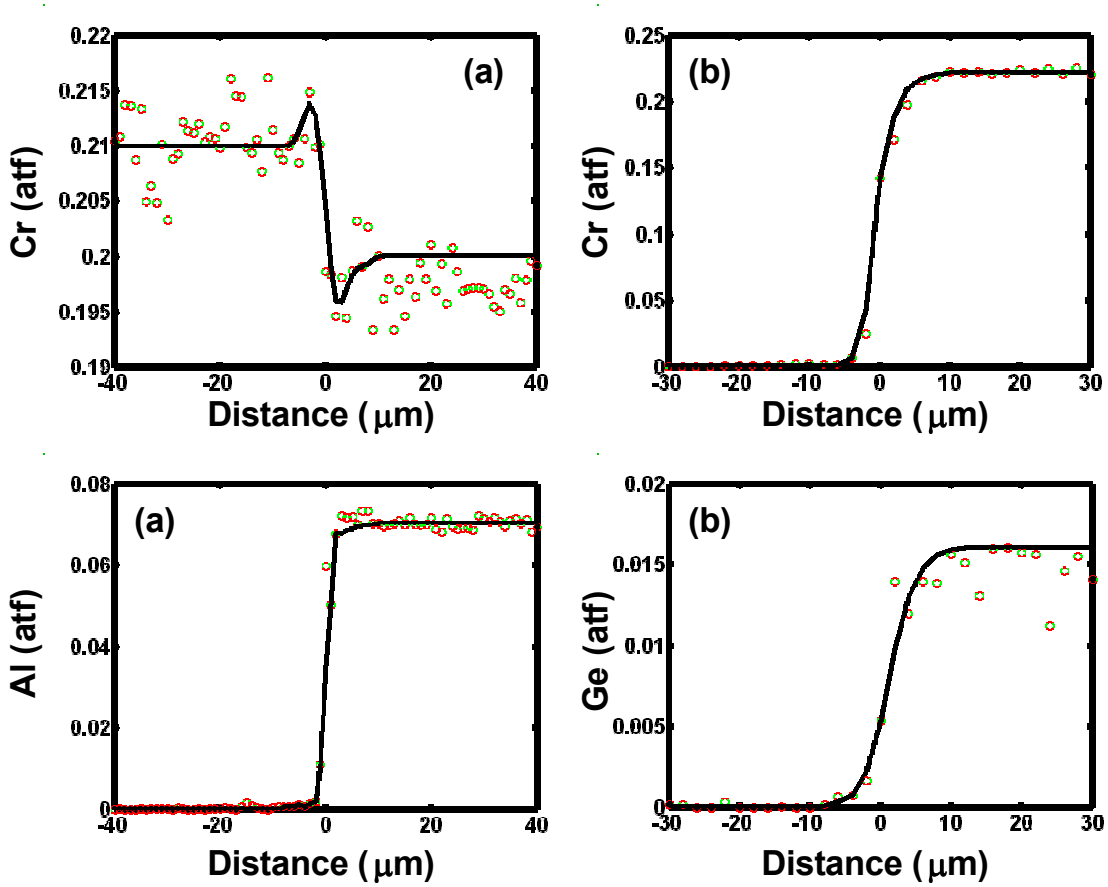

Fig. 2. Typical experimental and smoothened concentration profiles measured from solid-to-solid diffusion couples (a) Ni-Cr vs. Ni-Cr-Al and (b) Ni vs. Ni-Cr-Ge annealed at 700°C for 720 hours. Note that concentration is given in atf, which stands for atomic fraction.

Table 3. Average effective interdiffusion coefficients determined from Ni vs. Ni-Cr-X diffusion couples annealed at 700°C for 720 hours.

Diffusion Couple	Composition Range	$\tilde{D}^{eff}_{Cr}$ [10^{-18} m^2/s]	$\tilde{D}^{eff}_{X}$ [10^{-18} m^2/s]	$\tilde{D}^{eff}_{Ni}$ [10^{-18} m^2/s]
Ni vs. Ni-Cr (X = None)	$(C_i^{-\infty} \sim C_i^{o})$	1.98	-	1.98
	$(C_i^{o} \sim C_i^{+\infty})$	2.34	-	2.34
Ni vs. Ni-Cr-Al (X = Al)	$(C_i^{-\infty} \sim C_i^{o})$	0.50	0.40	0.47
	$(C_i^{o} \sim C_i^{+\infty})$	0.61	0.86	0.68
Ni vs. Ni-Cr-Si (X = Si)	$(C_i^{-\infty} \sim C_i^{o})$	1.22	2.08	1.27
	$(C_i^{o} \sim C_i^{+\infty})$	1.95	2.26	1.99
Ni vs. Ni-Cr-Ge (X = Ge)	$(C_i^{-\infty} \sim C_i^{o})$	1.39	2.38	1.43
	$(C_i^{o} \sim C_i^{+\infty})$	2.74	5.17	2.97
Ni vs. Ni-Cr-Pd (X = Pd)	$(C_i^{-\infty} \sim C_i^{o})$	6.91	6.06	6.85
	$(C_i^{o} \sim C_i^{+\infty})$	9.86	5.41	9.57

Using Eq. 3, average effective interdiffusion coefficients, $\tilde{D}_i^{eff}$'s on either side of the Matano plane were determined from the concentration profiles obtained from series I and II diffusion couples (i.e., Ni vs. Ni-Cr and Ni vs. Ni-Cr-X). They are reported in Table 3. These average effective interdiffusion coefficients are two orders lower in magnitude than those determined at 900°C [9]. $\tilde{D}_i^{eff}$ was generally higher on the $\left(C_i^o \sim C_i^{+\infty}\right)$ composition range with higher Cr concentration relative to the other side.

Table 3 also reports that Al, Si and Ge diffuse faster than Ni in γ-phase Ni-Cr-X alloys. In the case of Ni vs. Ni-Cr-Pd, $\tilde{D}_i^{eff}$'s for Ni, Cr and Pd are similar. These results are in general, analogues to previous work [9] carried out at 900°C. At 700°C, Table 3 shows that Al and Si additions to Ni-Cr alloy reduced $\tilde{D}_{Cr}^{eff}$, but Pd additions to Ni-Cr alloy increased $\tilde{D}_{Cr}^{eff}$ significantly, especially in the composition range of $\left(C_i^o \sim C_i^{+\infty}\right)$.

Concentration profiles obtained from diffusion couple series II and III (i.e., Ni vs. Ni-Cr-X and NiCr vs. Ni-Cr-X) were employed to determine average ternary interdiffusion coefficients, $\overline{\tilde{D}}_{ij}^{Ni}$ on either side of the Matano plane using Eq. 5. These are reported in Table 4 and 5. The magnitude of these interdiffusion coefficients is approximately two orders lower than those determined at 900°C [9]. The sign of the cross interdiffusion coefficients remained the same with those determined at 900°C.

Series II diffusion couples were designed to yield the same sign of $\partial C_{Cr}/\partial x$ and $\partial C_X/\partial x$ where a positive and negative $\overline{\tilde{D}}_{CrX}^{Ni}$ indicates an increase and a decrease in $\tilde{J}_{Cr}$, respectively. In general, higher magnitude of $\overline{\tilde{D}}_{CrCr}^{Ni}$ and $\overline{\tilde{D}}_{XX}^{Ni}$ was observed on the $\left(C_i^o \sim C_i^{+\infty}\right)$ composition range with higher Cr concentration. The Al addition in the Ni-Cr alloy yielded positive $\overline{\tilde{D}}_{CrAl}^{Ni}$, and increased $\tilde{J}_{Cr}$ in agreement with the previous work by Nesbitt [14], Thomson [15] and Garimella [9].

Table 4. Average ternary interdiffusion coefficients determined from Ni-Cr vs. Ni-Cr-X diffusion couples annealed at 700°C for 720 hours.

Diffusion Couple	Composition Range	$\overline{\tilde{D}}_{CrCr}^{Ni}$ [10^{-18} m^2/s]	$\overline{\tilde{D}}_{CrX}^{Ni}$ [10^{-18} m^2/s]	$\overline{\tilde{D}}_{XCr}^{Ni}$ [10^{-18} m^2/s]	$\overline{\tilde{D}}_{XX}^{Ni}$ [10^{-18} m^2/s]
Ni vs. Ni-Cr-Al (X = Al)	$\left(C_i^{-\infty} \sim C_i^o\right)$	0.48	0.53	0.06	0.42
	$\left(C_i^o \sim C_i^{+\infty}\right)$	0.54	0.02	0.10	0.35
Ni vs. Ni-Cr-Si (X = Si)	$\left(C_i^{-\infty} \sim C_i^o\right)$	0.96	0.58	0.03	1.20
	$\left(C_i^o \sim C_i^{+\infty}\right)$	1.42	0.05	0.05	1.30
Ni vs. Ni-Cr-Ge (X = Ge)	$\left(C_i^{-\infty} \sim C_i^o\right)$	0.67	5.44	Negligible	2.51
	$\left(C_i^o \sim C_i^{+\infty}\right)$	0.93	5.84	Negligible	2.88
Ni vs. Ni-Cr-Pd (X = Pd)	$\left(C_i^{-\infty} \sim C_i^o\right)$	6.49	4.92	Negligible	5.84
	$\left(C_i^o \sim C_i^{+\infty}\right)$	7.59	5.83	Negligible	5.58

The Si, Ge and Pd additions to Ni-Cr alloy also increased $\tilde{J}_{Cr}$ with positive $\overline{\tilde{D}}_{CrX}^{Ni}$. This effect was stronger when Cr concentration was high on the $\left(C_i^o \sim C_i^{+\infty}\right)$ side particularly for Ge and Pd. In previous work at 900°C [9], $\overline{\tilde{D}}_{CrGe}^{Ni}$ was not significant to this extent. The Si, Ge and Pd additions to

Ni-Cr alloy also increased $\tilde{J}_{Cr}$ with positive $\overline{\tilde{D}}^{Ni}_{CrX}$. This effect was stronger when Cr concentration is high on the $\left(C_i^o \sim C_i^{+\infty}\right)$ side, particularly for Ge and Pd. In previous work at 900°C [9], $\overline{\tilde{D}}^{Ni}_{CrGe}$ was not significant while $\overline{\tilde{D}}^{Ni}_{CrSi}$ and $\overline{\tilde{D}}^{Ni}_{CrPd}$ were significantly large. This study at 700°C finds that $\overline{\tilde{D}}^{Ni}_{CrGe}$ and $\overline{\tilde{D}}^{Ni}_{CrPd}$ are large positive values while $\overline{\tilde{D}}^{Ni}_{CrSi}$ is not so significant.

Diffusion couple series III was designed so that the initial $\partial C_{Cr}/\partial x \approx 0$. Therefore, $\tilde{J}_{Cr}$ is mainly due to $\partial C_X/\partial x$, and the magnitude and sign of $\overline{\tilde{D}}^{Ni}_{CrX}$. $\tilde{J}_{Al}$ and $\tilde{J}_{Si}$ have caused an uphill-diffusion of Cr owing to positive $\overline{\tilde{D}}^{Ni}_{CrAl}$ and $\overline{\tilde{D}}^{Ni}_{CrSi}$, respectively. On the other hand, $\tilde{J}_{Ge}$ and $\tilde{J}_{Pd}$ did not cause any measurable redistribution of Cr ($\tilde{J}_{Cr} \approx 0$). However, Ge and Pd are lower in concentration than those of Al and Si, in the Ni-Cr-X alloys, as reported in Table 1. Average ternary interdiffusion coefficients for series-III couples are reported in Table 5.

Table 5. Average ternary interdiffusion coefficients determined from Ni vs. Ni-Cr-X diffusion couples annealed at 700°C for 720 hours.

Diffusion Couple	Composition Range	$\overline{\tilde{D}}^{Ni}_{CrCr}$ [10^{-18} m^2/s]	$\overline{\tilde{D}}^{Ni}_{CrX}$ [10^{-18} m^2/s]	$\overline{\tilde{D}}^{Ni}_{XCr}$ [10^{-18} m^2/s]	$\overline{\tilde{D}}^{Ni}_{XX}$ [10^{-18} m^2/s]
Ni-Cr vs. Ni-Cr-Al (X = Al)	$\left(C_i^{-\infty} \sim C_i^o\right)$	1.98	0.73	1.97	0.78
	$\left(C_i^o \sim C_i^{+\infty}\right)$	2.65	1.00	1.01	0.76
Ni-Cr vs. Ni-Cr-Si (X = Si)	$\left(C_i^{-\infty} \sim C_i^o\right)$	6.91	5.87	0.11	0.62
	$\left(C_i^o \sim C_i^{+\infty}\right)$	2.59	2.22	0.16	1.35
Ni-Cr vs. Ni-Cr-Ge (X = Ge)	$\Delta C_{Cr}/\Delta x \approx 0$ and cannot be determined				
Ni-Cr vs. Ni-Cr-Ge (X = Ge)					

Based on average effective interdiffusion coefficients and average ternary interdiffusion coefficients determined in both the present study at 700°C and earlier study at 900°C [9], alloying additions of Al, Si, Ge and Pd have yielded positive $\overline{\tilde{D}}^{Ni}_{CrX}$. Therefore, Cr_2O_3-forming ability of Ni-22at.%Cr alloy should improve with these alloying additions.

Summary

Experimental concentration profiles, measured after annealing at 700°C for 720 hours, were employed to determine interdiffusion fluxes, average effective interdiffusion coefficients and average ternary interdiffusion coefficients. The, $\overline{\tilde{D}}^{Ni}_{CrX}$ were observed to be positive with the alloying additions of Al, Si, Ge, or Pd. These results indicate that these alloying additions can facilitate the formation of Cr_2O_3-scale after scale-spallation and Cr-depletion due to long-term oxidation.

Acknowledgements

This work was supported by the NSF CAREER Award under the grant DMR-0238356.

References

[1] J.L. Smialek and G.H.Meier, in: High temperature oxidation, edited by C.T. Sims, N.S. Stoloff, and W.C. Hagel, of Superalloy II, chapter 11, John Weley & Sons (1987).

[2] P. Kofsted, in: Growth and protective properties of Chromia (Cr_2O_3) and Alumina (Al_2O_3) scales, protective coatings, of High temperature Corrosion, Elsevier,London (1980) p. 389-404.

[3] J.L. Smialek, C.A. Barrett, J.C. Schaffer, in: Design for oxidation resistance, edited by George E. Dieter,Vol. 20 of ASM handbook, ASM International (1997).

[4] F.H. Stott, G.C. Wood, and J.Stringer : Oxi. Metals, Vol. 44 (1995), p. 113-145.

[5] D.P.Whittle and J.Stringer: Proc. R. Soc. Lond., Ser. A, Vol. 295 (1980), p.309-329.

[6] G.C. Wood and F.H.Stott: Mater. Sci. Technol., Vol.3 (1987), p. 519-530.

[7] W.C.Hagel: Corrosion, Vol. 21 (1965), p. 316-326.

[8] J.A. Nesbitt: Oxid. Metals, Vol. 44 (1995), p 309-338.

[9] N.Garimella, M.P. Brady and Y.H.Sohn: Journal of Phase Equilibria and Diffusion, Vol. 27, (2006), p. 665-670.

[10] L.Onsager, Ann. N.Y.Acad. Sci., Vol. 46 (1965), p. 241-265.

[11] M.A. Dayananda and C.W.Kim: Metall. Trans. A, Vol. 10A (1979), p. 1333-1339.

[12] M.A. Dayananda and Y.H.Sohn: Scr. Mater., Vol. 40 (1996), p. 683-688.

[13] M.A. Dayananda and Y.H.Sohn: Metall. Trans. A, Vol. 30A (1999), p 535-543.

[14] J.A. Nesbitt and R.W. Heckel: Metall. Trans. A, Vol.18A (1987), p 2075-2086.

[15] M.S.Thomson, J.E.Morral, and A.D.Roming Jr.: Metall. Trans. A, Vol. 21A, (1990), p. 2679-2685.